

Wavelength demultiplexers based on multimode interference effect in photonic crystals

Z.H. Zhu^{*}, W.M. Ye, J.R. Ji, X.D. Yuan, C. Zen

College of Opto-Electronic Engineering, National University of Defense Technology, Changsha 410073, Hunan, PR China

Received 18 April 2007; received in revised form 18 September 2007; accepted 1 December 2007

Available online 14 December 2007

Communicated by R. Wu

Abstract

We present a compact photonic crystal wavelength demultiplexing device based on multimode interference effect. The finite-difference time-domain method is used to verify and analyze the characteristics of the device. Results show the demultiplexing function of the device can be obtained with greater than 20 dB isolation ratio and about 20 nm bandwidth at both wavelength bands.

© 2007 Elsevier B.V. All rights reserved.

PACS: 42.70.Qs; 42.79.Ci

1. Introduction

One essential components of photonic integrated circuits are wavelength demultiplexers. These wavelength demultiplexing devices are used to separate several optical channels at different wavelengths with key features being compactness and low cross-talk. Due to lack of an appropriate optical material with high dispersive properties to reduce the device size, wavelength demultiplexing devices with required properties for practical applications have not been realized yet. Fortunately, photonic crystals [1,2] opens a new opportunity for this critical issue because of its capability to confine the electromagnetic wave within a small size [3,4]. Therefore, many researchers seek their new ways of wavelength demultiplexing using photonic crystals [5–7]. The superprism effect [8] and the directional coupling [9] in photonic crystals have also been demonstrated to realize of wavelength demultiplexing, respectively. Recently, because of their simple structure, ease of fabrication, low loss and large optical bandwidth, Photonic crystal multimode interference (MMI) [10] devices of wavelength demultiplexing have also been proposed [11]. However, in this type of device, photonic crystal structure is only a assisted part, which

provides the reflectivity and/or transmission by bandgap of photonic crystals.

In this Letter, we propose a photonic crystal MMI configuration consisting of three simple-mode waveguides and one multimode region to obtain wavelength demultiplexing. For proof of principle purposes, we demonstrate by finite-difference time-domain (FDTD) simulation that this concept holds for photonic crystals formed by dielectric rods in air.

2. Design and analysis

As photonic band-gap (PBG) system, we consider a square lattice of dielectric rods in air, as shown in Fig. 1(a). We choose the relative dielectric constant and the radius of the rods to be $\epsilon_r = 11.56$ (InGaAsP–InP material system) and $r = 0.18a$, respectively, where a is the lattice constant. For TM mode with the electric field parallel to the rod axis, the photonic bandgap of the PC structure is calculated by the plane wave expansion (PWE) method and can be found in the normalized frequency range between 0.302 and 0.443 ($\omega a/2\pi c$), where ω and c are the angular frequency and the light velocity in vacuum, respectively. All results presented are for TM mode and have been obtained with the 2D FDTD with perfectly matched layer boundary condition. The simulations use 20×20 grid points per unit cell.

^{*} Corresponding author.

E-mail address: nudtzzh@hotmail.com (Z.H. Zhu).

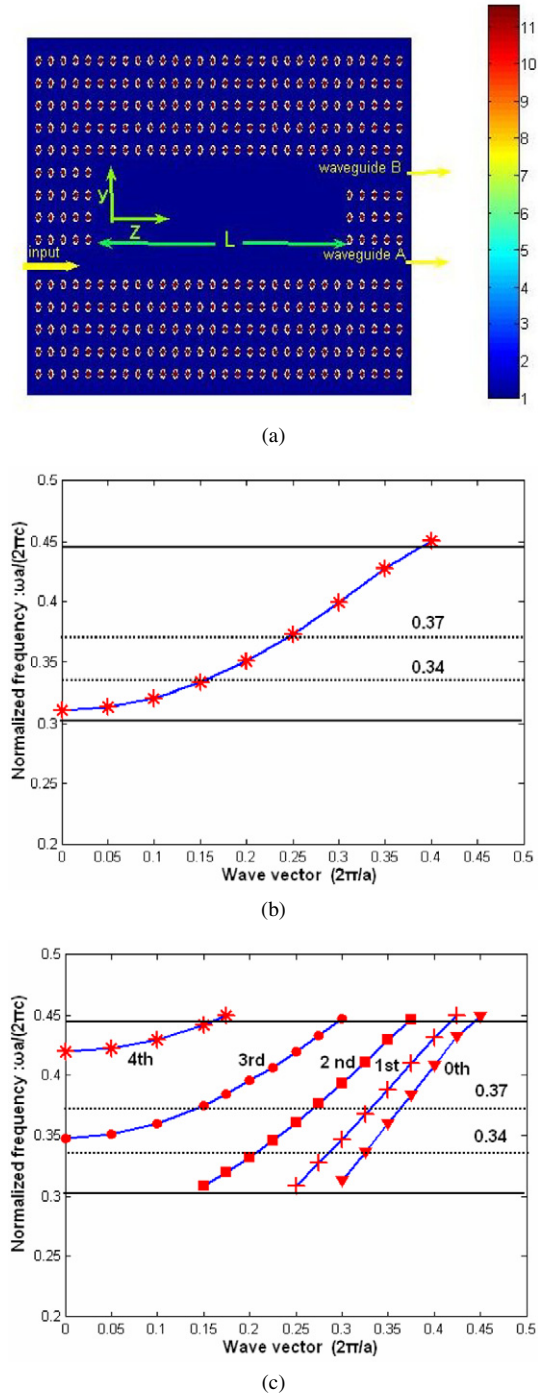


Fig. 1. Model of the proposed MMI wavelength demultiplexing structures. (a) Relative dielectric constant distributions by our 2D FDTD calculation. The structure consists of three simple-mode waveguides and one multimode waveguide, created by removing one row and five rows of the air holes, respectively. L is the length of the multimode region. (b) Dispersion curves for simple-mode waveguide. (c) Dispersion curves for multimode waveguide.

Fig. 1 shows the structure of the wavelength demultiplexing devices. The structure consists of three simple-mode waveguides and one multimode waveguide, created by removing one row and five rows of the air holes, respectively. As shown in Fig. 1(a), simple-mode waveguides function as input and output waveguides (waveguide A and waveguide B),

while multimode waveguide serves as the MMI region. To confirm the number of guided modes supported by the input/output waveguide and multimode region, dispersion curves for the two types of photonic crystal waveguides are calculated by FDTD method. The results are shown in Fig. 1(b) and (c), which correspond to the dispersion curves of guided modes in the input/output waveguide and multimode region, respectively. From Fig. 1(b), we can see that the input/output waveguide hold one mode within the bandgap of photonic crystals and therefore ensure single-mode propagation, while the multimode region holds five modes. For proof of principle purposes, we choose randomly two frequencies 0.34 and 0.37 ($\omega a / 2\pi c$) to demonstrate the wavelength demultiplexing.

After launching an input signal including two frequency components 0.34 and 0.37 ($\omega a / 2\pi c$) into the waveguide A, in the multimode regions three and four guided modes are excited by the input frequency components 0.34 and 0.37, respectively. So the total field $\psi(y, z)$ in the multimode region is given by a superposition of all guided modes [10]:

$$\psi(y, z) = \psi_1(y, z) + \psi_2(y, z) = \sum_{n=0}^2 c_{1,n} \phi_{1,n}(y) e^{-j\beta_{1,n}z} + \sum_{m=0}^3 c_{2,m} \phi_{2,m}(y) e^{-j\beta_{2,m}z}, \quad (1)$$

where ψ_1 denotes the field of the frequency component 0.34, and $c_{1,n}$, $\phi_{1,n}$ and $\beta_{1,n}$ denote the excitation coefficient, modal field distribution and propagation constant of the n th mode of the frequency component 0.34, respectively. ψ_2 , $c_{2,m}$, $\phi_{2,m}$ and $\beta_{2,m}$ correspond to the frequency component 0.37. For simplicity, the initial phase of the input field at $z = 0$ is assumed to be 0, and therefore the input field at $z = 0$ should be

$$\psi(y, 0) = \psi_1(y, 0) + \psi_2(y, 0) = \sum_{n=0}^2 c_{1,n} \phi_{1,n}(y) + \sum_{m=0}^3 c_{2,m} \phi_{2,m}(y). \quad (2)$$

The total field profile at a distance L can be written as

$$\psi(y, L) = \sum_{n=0}^2 c_{1,n} \phi_{1,n}(y) e^{-j\beta_{1,n}L} + \sum_{m=0}^3 c_{2,m} \phi_{2,m}(y) e^{-j\beta_{2,m}L}. \quad (3)$$

When L_d satisfy

$$\beta_{1,n} L_d = (2k_{1,n} + 1)\pi \quad (k_{1,n} = 0, 1, 2, \dots) \quad (4)$$

$$\text{and } \beta_{2,m} L_d = 2k_{2,n}\pi \quad (k_{2,n} = 1, 2, 3, \dots). \quad (5)$$

Eq. (3) can be written as [12]

$$\psi(y, L_d) = \psi_2(y, 0) + \psi_1(-y, 0). \quad (6)$$

Eq. (6) denotes that a direct image of the input field of the frequency component 0.37 ($\omega a / 2\pi c$) and a mirrored one for the frequency component 0.34 ($\omega a / 2\pi c$) are reproduced at $z = L_d$, which imply the demultiplexing function for the frequencies

Download English Version:

<https://daneshyari.com/en/article/1866228>

Download Persian Version:

<https://daneshyari.com/article/1866228>

[Daneshyari.com](https://daneshyari.com)